Available online at www.sciencedirect.com
ScienceDirect
Trans. Nonferrous Met. Soc. China 21(2011) s523−s528
Transactions of Nonferrous Metals Society of China
www.tnmsc.cn

Quick image-processing method of UAV without control points data in earthquake disaster area

LI Chang-chun[1], ZHANG Guang-sheng[1], LEI Tian-jie[2, 3], GONG A-du[2, 3]

1. School of Surveying & Land Information Engineering, Henan Polytechnic University, Jiaozuo 454000, China;
2. Key Laboratory of Environmental Change and Natural Disaster, Ministry of Education, Beijing Normal University, Beijing 100875, China;
3. Ministry of Civil Affairs/Ministry of Education of China Academy of Disaster Reduction and Emergency Management, Beijing Normal University, Beijing 100875, China

Received 19 June 2011; accepted 10 November 2011

Abstract: The methods of unmanned aerial vehicles images splicing rapidly and rectifying without control points data, only using auxiliary data recorded by unmanned aerial vehicle (UAV) system, were researched. Two algorithms were proposed, including UAV images auto- splicing rapidly after image blocking and UAV images rectifying based on pseudo center points of auxiliary data. When SIFT algorithm for UAV images splicing is applied, the accuracy is very high, but the efficiency is very low. The splicing efficiency is improved greatly based on SIFT algorithm after image blocking. The results show that rectifying accuracy is very high and has no visual dislocation when pseudo center points of auxiliary data is applied.

Key words: unmanned aerial vehicles; SIFT algorithm; blocking; quickly splicing; rectification

1 Introduction

As an important means of obtaining spatial data, the unmanned aerial vehicle (UAV) remote sensing has such advantages as real-time, flexiblility, high-resolution, low cost, and it can collect information in dangerous environments without risk [1−3]. So, it is very suitable for emergency monitoring and reconstruction of all types of disasters, especially the use of on-site emergency response. It can greatly enhance the capability of data collection and data transmission on-site for disaster emergency working group. But our country does not have a sophisticated UAV image processing system, and the corresponding image processing software is also very rare.

At present, the flow of UAV image processing is based on traditional photogrammetric methods [4−5], the results, accuracy is relatively high, while the demand for original data is quite harsh. So, high-precision attitude parameters and ground control point (GCPs) data must be acquired. However, it is difficult to meet the demand of traditional aerial triangulation because the flight quality of UAV remote sensing system can be affected by low-flying. As a result, the image processing of UAV cannot use the traditional aerial photography methods. The GCPs data will be destroyed by earthquake, the algorithms of UAV image processing without GCPs data must be researched.

Subminiature UAV is adopted in the experiment, with low cost and is convenient to carry, but it is greatly affected by airflow when flying, and cannot record the attitude data. Because the experimental zone is in the earthquake area, accurate GCPs data cannot be captured. The methods of UAV image splicing and rectifying without GCPs are proposed. When splicing images, local invariant features is introduced, i.e., SIFT algorithm, which splicing accuracy is very high, but efficiency is very low [6−7]. The method of image auto-splicing after blocking is proposed, with a very high accuracy, furthermore, it can make full use of the existing data, so the efficiency is improved greatly.

Foundation item: Project(41071259)supported by National Natural Science Foundation in China
Corresponding author: LI Chang-chun; Tel: 13782827058; E-mail: lichangchun610@126.com

2 Pilot site and data-obtaining situation

2.1 Overview of pilot site

The flying experimental zone of UAV is Hanwang town of Sichuan Province which lies in the northeast of Sichuan basin, and mountains and hills are its main landform. The climate of this zone is tropical humid, so there is much cloud and humidity. The weather when flying is fine and the power of wind is gentle. The UAV flies along one side of a river valley, the zone of flying is very flat, and the average elevation is 660 m. The total area of flying zone is 35 km^2. The key parameters of UAV remote sensing platform and its sensor are shown in Tables 1 and 2.

Table 1 Main parameters of UAV remote sensing platform

Item	Value
Length/m	1.2
Flying height/m	400−1 000
Load/kg	4.5
Speed/(km·h^{-1})	70−110
Lasting period/min	60
Controlling way	Autocontrolling
Navigation way	GPS
Sensor	Digital camera

Table 2 Main parameters of UAV sensor

Item	Value
Image sensor	Liguang digital II
Resolution	10 000 000
Lens focal/mm	28
CCD size/m	(1/1.75)×304 8
File size/pixel	3 680×2 376
Record format	JPEG

2.2 Data-obtaining situation

The lateral overlap of images is 30%, the longitudinal overlap is 80%, and the flight height is 880 m. 3 456 images (the size of each image is 3 million Byte) are obtained in two flights, and each image has a group of auxiliary data. Table 3 shows the format of auxiliary data recorded by UAV, which includes image number, longitude and latitude recorded by GPS, speed, height and orientation angle.

3 Data analysis

3.1 Image data

The experimental image dada have the following features.

1) The frame of image is small and the number is large. The common non-metric digital camera is used, so the frame of image is small; at the same time, in order to get high resolution images, the flight height is low, so the coverage of each image is small.

The image resolution formula can be obtained referring to the 1:500, 1:1 000, 1:2 000 aerial photography standard [8], according to the relation of focus length, flight height and resolution, and the formula is as follows:

$$\frac{f}{H}=\frac{C}{A} \tag{1}$$

where f is the focus length; H is the flight height; C is the CCD size; A is the ground covering area, which can be calculated by A=pixel number×resolution.

The UAV sensor parameters are shown in Table 2. fixed focus model was proposed during shooting. The focus length is 5.9 mm, CCD size is 1/1.75, and image size is 3 648 pixel ×2 376 pixel.

The flight height is about 220 m according to the average elevation and recorded GPS elevation of experimental zone. Substituting data into Formula (1), the resolution R=0.08 m. Each image covers the area of 0.005 km^2.

Table 3 Auxiliary data recorded by UAV remote sensing system

No.	Latitude	Longitude	Speed/(m·s^{-1})	Height/m	Orientation angle
0001	31°27.235′	104°10.535′	V000	H0682	C140
0002	31°27.235′	104°10.534′	V000	H0682	C140
0003	31°26.984′	104°10.183′	V044	H0874	C143
0004	31°26.965′	104°10.202′	V043	H0872	C141
0005	31°26.946′	104°10.220′	V041	H0871	C142
⋮	⋮	⋮	⋮	⋮	⋮
3455	31°27.031′	104°10.496′	V051	H0887	C179
3456	31°27.002′	104°10.497′	V050	H0888	C178

Processing all the 3 000 images one by one will spend a large amount of time if normal processing method is adopted.

2) Flight track is irregular curve. Extract the point number and coordinates recorded by auxiliary data, import Excel table, open by ArcGIS software, output Shapefile model files in the end generating flight track, as shown in Fig. 1. The curve reflects flying tracks, where 1, 2, 3, ⋯ are the number of UAV images.

It can be seen from Fig. 1 that the flying track is irregular, which leads to the overlap of image variance, especially, the overlap rate is more different between two images in the lateral direction.

3) Large image deforming. Because of using non-metric common digital camera, the flight attitude is not stable, as shown in Table 3. The projecting relation between single image and ground object space is complex, the camera len distortion is very large, and the geometrical relation of images is not stable. The slant deformation of images is large, the light and shade contrast degree between images is different. At the same time, the fluctuation of ground affects the resolution because of the low altitude flight.

3.2 Auxiliary data

Because of the limit of payload and cost of the UAV, the accuracy of the GPS fixed on UAV is about 10 m, and the coordinates of the GPS point recorded by the auxiliary data are not located in the image centers. The accuracy of orientation angles is only degree.

For this experiment, there are no other control points data except for images and coordinates from Google Earth. And it is difficult to get new data after earthquake and the resolution of the GoogleEarth data is low, only the rivers and buildings can be identified.

4 UAV images processing

For the above reasons, traditional photogrammetric method cannot be utilized when dealing with the UAV images. At the same time, the absolute positioning accuracy of UAV images is not of the first importance in disaster. What we really want is disaster alert, relief and assessment and to get orthoimages or quasi orthoimages of the regions and the area of different land types.

Because control points data cannot be obtained, the image processing method without control points data is proposed. The method includes three steps: The first one is automatic splicing; the second one is rectification; the last one is mosaic. After above steps, rectifying images in all flight regions can be gotten quickly, and basic is provided for the following ortho-rectification and classification.

4.1 Auto-splicing of images

At present, there are two UAV images splicing methods [9−11]: The simple one is based on coordinates which are usually from attitude parameters or control points data, but they are not easy to be got or their accuracy is poor. The other method is based on image

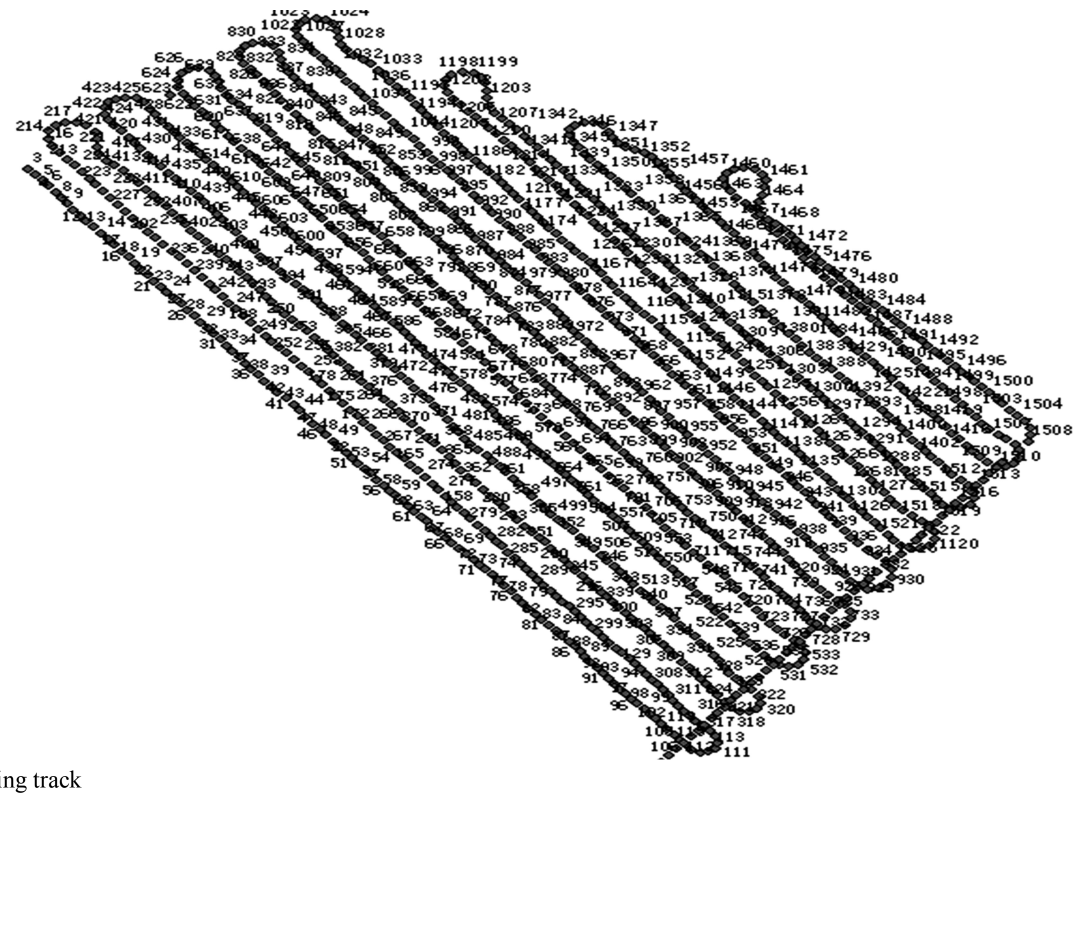

Fig. 1 Flying track

feature matching, which includes correlative index, wavelet, SITT, Fourier transformation, etc.

Because of the large quantity of data and owning only some auxiliary data recorded when flying, the strategy is to automatically splice the small original images using image matching algorithm. The blocks of image will be rectified based on the auxiliary data after splicing. As the longitudinal overlap is 80%, in order to improve speed and obtain the whole aerial image as quickly as possible, one image is chosen every two images in the direction which can guarantee overlap ratio (the maximum overlap ratio is 80%×80%× 80%) and improve processing speed as well.

Firstly, the optimal number of rows and columns automatic spliced in small area should be decided according to experiment. The criteria of deciding include splicing result accuracy and efficiency. According to many experiments, 15×5 (longitudinal direction and lateral direction are 15 and 5 respectively) is most preferred which efficiency is the highest. At the same time, in order to improve splicing result between blocks, the overlap degree between blocks also should keep at about 35%. Then the small blocks are automatic spliced, and the splicing result can be improved by fine tuning the image number and overlap degree. The whole processing flow is shown in Fig. 2.

The automatic matching process adopts SIFT algorithm, which can extract the local features of the image, keep invariance property while rotating, zooming and changing luminosity, also keep some stability for visual angle changing, and affine transformation and noise. At the same time, the method can match images quickly and accurately from a large number of feature database, therefore, it is fit for the UAV image matching, of which amount is great and deformation is large.

The steps of SIFT feature matching are as follows [12−14]: First one is establishing different scale space,

$$G(x,y,\sigma)=\frac{1}{2\pi\sigma^2}\exp[-(x^2+y^2)/(2\sigma^2)] \tag{2}$$

$$L(x,y,\sigma)=G(x,y,\sigma)*I(x,y) \tag{3}$$

where (x, y) represents point coordinates; σ is scale space, $G(x, y, \sigma)$ is Gaussian function; $L(x, y, \sigma)$ is scale space; "*" represents convolution operation. The different scale spaces will be established with the change of parameter σ.

In Fig. 3, s is different samplings of the scale space. After establishing the scale space, the point can be positioned accurately using Gaussian difference algorithm. The point with the surrounding eight points and the corresponding position points of adjacent scale were compared to confirm whether it was a feature point. When the feature points are decided, the direction parameters of each point can be appointed through making use of the gradient direction distributing features of its neighborhood pixels, which can keep the feature of rotate invariance.

After SIFT matched features were established, the following is to determine the similarity of these features. Find a feature point from the first image, then two points from the second image, between which Euclidean distance is the nearest. If the ratio that the smallest distance is divided by the secondary one is smaller than the threshold, this point will match the nearest one successfully. As shown in Fig. 4, the two ends of lines are the matching point pairs.

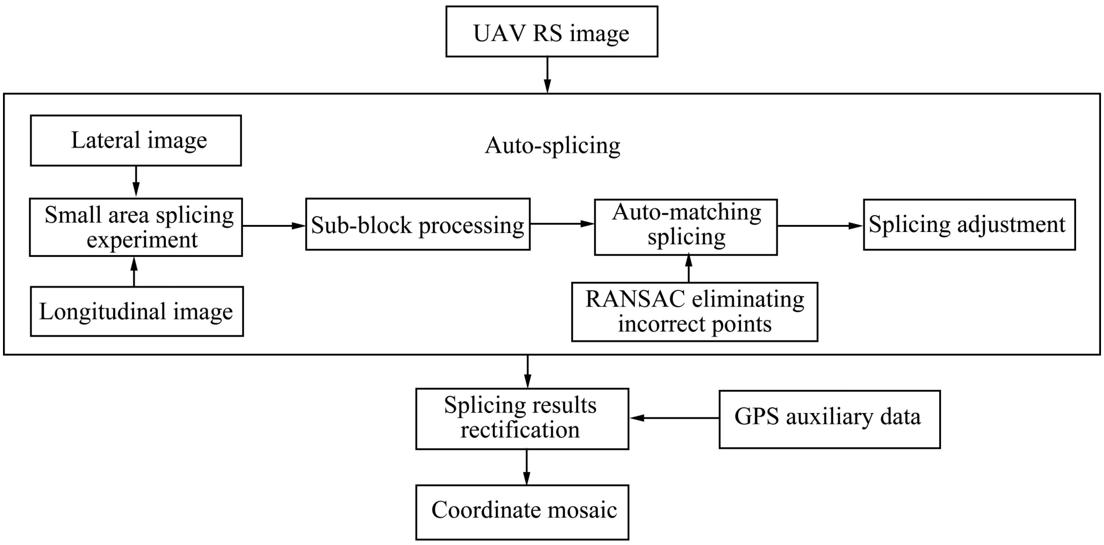

Fig. 2 Flow chart of image processing

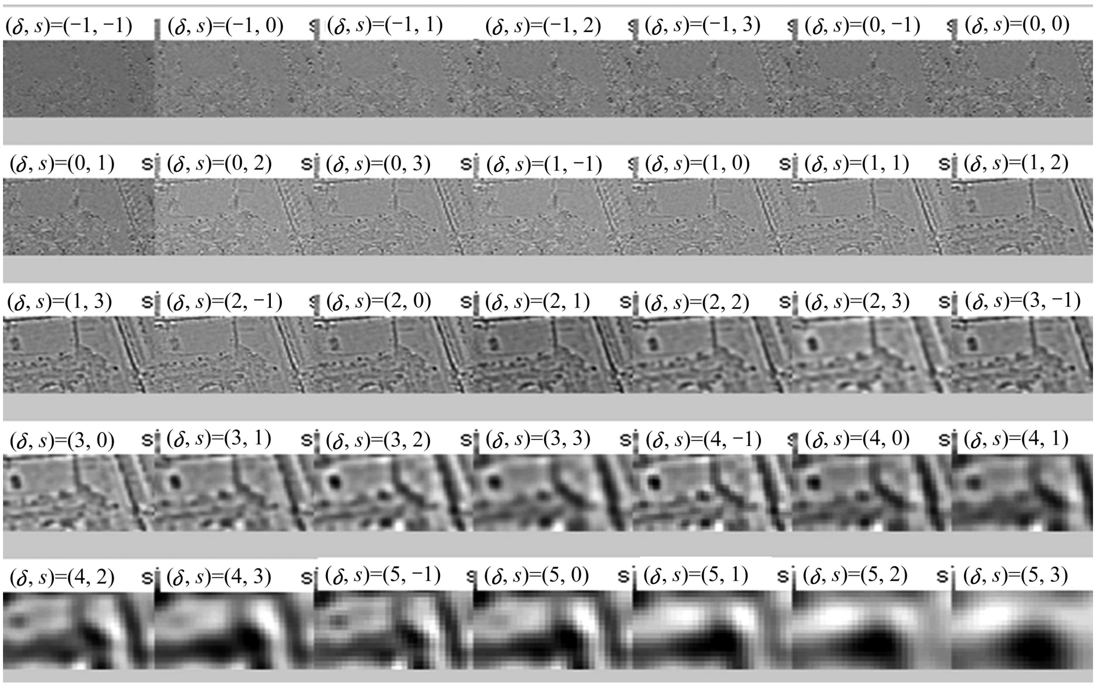

Fig. 3 Image characters in different scale spaces

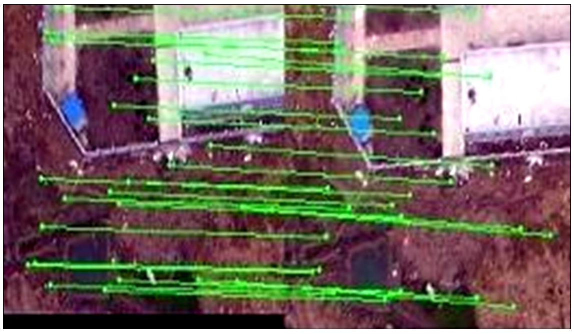

Fig. 4 Results of feature points matching

By taking RANSAC algorithm [15−16] to delete incorrect points, keeping at least four pairs matching points, the bilinear transformation matrix will be established:

$$\begin{aligned} X &= a_1 x + b_1 y + c_1 xy + d_1 \\ Y &= a_2 x + b_2 y + c_2 xy + d_2 \end{aligned} \tag{4}$$

According to the calculated transformation matrix parameters, the adjacent images can be spliced. For the rectifying result shown in Fig. 6, the transformation matrix calculated by two images is as follows:

$$\boldsymbol{M} = \begin{bmatrix} 0.999168 & -0.0386002 & 0.000131057 & 527.8177 \\ 0.0386011 & 0.999255 & -0.000200111 & -34.324655 \end{bmatrix} \tag{5}$$

It can be found from the matrix that the zooming distortion between images is very small, but has some degree rotating distortions.

4.2 Images rectifying and mosaic

The spliced images can be rectified by using auxiliary data recorded by airborne GPS. The point positions recorded by GPS are not the image center; however in the same direction, the relative position between GPS and camera keeps unchanged, so the points recorded by GPS can be regarded as pseudo center points. The points of upperleft flying direction are used to correct in this experimental. Image before rectifying is shown in Fig. 5. The rectifying result is shown in Fig. 6. It can be found from Fig. 6 that the splicing of the main factors, such as roads and rivers, are perfect, and has no vision misplacement.

The images after rectified have coordinate information, which will be easy to splice. After mosaicing those corrected blocks into a large map, it can provide data source for classification and ortho-correction.

Fig. 5 Image before rectifying

Fig. 6 Result of rectifying

5 Conclusions

The fast image-processing method only using the auxiliary data recorded by UAV system without other control point data has been explored. The purpose is to splice the image automaticly with the data recorded by the UAV system, so as to realize the image rectifying in large area.

Firstly, the data is divided into several fine blocks based on the flight track; then SIFT algorithm is used to image splice automaticly with high accuracy and efficiecy; at last, the blocked images can be rectified by analyzing the pseudo center points of the auxiliary data.

The splicing and rectifying for all data of this experiment can be finished within 2 d, the whole mosaic image of the experimental area has high accuracy without vision misplacement.

Quantitative analysis of the splicing accuracy has not been made because of data limit, which is important for result to apply.

References

[1] CUI Hong-xia, LIN Zong-jian, SUN Jie. Research on UAV remote sensing system [J]. Bulletin of Surveying and Mapping, 2005(5): 11−14. (in Chinese)

[2] KIM J H, LEE D W, CHO K R, JO S Y. Development of an electro-optecal system for small UAV [J]. Aerospace Science and Technology, 2010, 14(7): 505−511.

[3] YEW C P, GARY B. Development and application of an integrated framework for small UAV flight control development [J]. Mechatronic, 2010, 21(5): 789−802.

[4] CUI Hong-xia, LIN Zong-jian, SUN Jie. The study of three dimensional modeling based on big overlapping UAV images [J]. Science of Surveying and Mapping, 2005, 30(2): 37−39. (in Chinese)

[5] XIANG Hai-tao, LEI Tian. Method for automatic georeferencing aerial remote sensing images from an unmanned aerial vehicle(UAV) platform [J]. Biosystem Engineering, 2011, 108(2): 104−113.

[6] LI Can-lin, MA Li-zhuang. A new framework for feature descriptor based on SIFT [J]. Pattern Recognition Letters, 2009, 30(5): 544−557.

[7] LOWE D G. Image feature from scale-invariant keypoints [J]. International Journal of Computer Vision, 2004, 60(2): 91−110.

[8] GB/T 6962—2005, 1:500 1:1 000 1:2 000 aerial photogrammetric standard[S]. Beijing: State Standardization Publishing House, 2005. (in Chinese)

[9] DI Ying-chen, CHEN Yun-ping, CHEN Ying-ying, CHEN Yan. Survey on image mosic algorithm of unmanned aerial vehicle [J]. Journal of Computer Application, 2011, 31(1): 170−174. (in Chinese)

[10] WANG Bin, WANG Wei-feng. Unmanned aerial vehicle image mosaic algorithm bases on local gray fitting [J]. Journal of China University of Petroleum, 2009, 33(2): 169−172. (in Chinese)

[11] CHENG Yuan-hang, XUE Ding-yu, HAN Xiao-wei. Fast image mosaic based on wavelet transform for remote sensing [J]. Journal of Northeastern University: Nature Science, 2008, 29(10): 1385−1388. (in Chinese)

[12] LOWE D G. Distinctive image features from scale-invariant interest points [J]. International Journal of Computer Vision, 2004, 60(2): 91−110.

[13] WANG Guo-mei, CHEN Xiao-wei. The study of SIFT algorithm [J]. Journal of Yang Cheng Institute of Technology, 2007, 20(2): 1−5. (in Chinese)

[14] LI Xiao-ming, ZHENG Lian, HU Zhan-yi. SIFT based automatic registration of remotely sensed imagery [J]. Journal of Remote Sensing, 2006, 10(6): 885−892. (in Chinese)

[15] ZHANG Xiao-hong, LI Bo, YANG Dan. A novel Harris multiscale corner detection algorithm [J]. Journal of Electronics and Information Technology, 2007, 29(7): 1735−1738. (in Chinese)

[16] HUNG You-qun, FU Yu, MA Guang-kun. Cylindrcal panoramic image stiching method based on RANSAC algorithm [J]. Journal of Shengyang University of Technology, 2008, 30(4): 461−465. (in Chinese)

(Edited by CHEN Can-hua)